VIP Aldehyde Peptide Synthesis Very Important Paper

International Edition: DOI: 10.1002/anie.201901589
German Edition: DOI: 10.1002/ange.201901589

Synthetic Lugdunin Analogues Reveal Essential Structural Motifs for Antimicrobial Action and Proton Translocation Capability

*Nadine A. Schilling, Anne Berscheid, Johannes Schumacher, Julian S. Saur, Martin C. Konnerth, Sebastian N. Wirtz, José M. Beltrán-Beleña, Alexander Zipperer, Bernhard Krismer, Andreas Peschel, Hubert Kalbacher, Heike Brötz-Oesterhelt, Claudia Steinem, and Stephanie Grond**

Dedicated to Professor Axel Zeeck on the occasion of his 80th birthday

Abstract: *Lugdunin, a novel thiazolidine cyclopeptide, exhibits micromolar activity against methicillin-resistant Staphylococcus aureus (MRSA). For structure–activity relationship (SAR) studies, synthetic analogues obtained from alanine and stereo scanning as well as peptides with modified thiazolidine rings were tested for antimicrobial activity. The thiazolidine ring and the alternating* D- *and* L-*amino acid backbone are essential. Notably, the non-natural enantiomer displays equal activity, thus indicating the absence of a chiral target. The antibacterial activity strongly correlates with dissipation of the membrane potential in S. aureus. Lugdunin equalizes pH gradients in artificial membrane vesicles, thereby maintaining membrane integrity, which demonstrates that proton translocation is the mode of action (MoA). The incorporation of extra tryptophan or propargyl moieties further expands the diversity of this class of thiazolidine cyclopeptides.*

Infectious diseases caused by antibiotic-resistant bacteria are an increasing health problem worldwide, especially the fast dissemination of MRSA.[1] As novel antibiotic entities have rarely been discovered in the last decade, we have an urgent need to find new structures. Numerous peptides such as daptomycin add to the great structural diversity of pharmaceutical agents. Modifications of peptide antibiotics are achieved by insertion of particular moieties, for example, double bonds or heterocycles, into the backbone structure. The cyclopeptide callyaerin and one of its analogues differ by a double bond, which confers constraints that correlate directly with their activity.[2] Notably, five- and six-membered carbocycles within the backbone mimic conformationally restricted β- and γ-amino acids.[3] Naturally occurring heterocycles also determine the structural flexibility of peptide macrocycles.[4] Interestingly, thiazolidine rings have not been reported as cyclopeptide components so far. During a screening approach for antibiotics using human bacterial nasal isolates,[5] lugdunin (**1**, Scheme 1) was discovered.[6] **1** is a nonribosomal cyclic peptide produced by *Staphylococcus lugdunensis* and features a thiazolidine ring as part of the backbone. **1** shows potent antimicrobial activity against pathogenic bacteria such as MRSA with a minimum inhibitory concentration (MIC) of 3.1 $\mu g\,mL^{-1}$ (3.9 μM). Furthermore, **1** mediates bactericidal effects when applied to mice after skin infection by *S. aureus*. However, the mode of action (MoA) of **1** has remained elusive.

We previously established the synthesis of **1** for the structural proof of natural lugdunin.[6] Now we present a comprehensive structure–activity relationship (SAR) study to identify the essential motifs of **1** for its antimicrobial activity. Derivatives of **1** were produced by solid-phase peptide synthesis (SPPS) on an aldehyde-generating resin. After assembly of the peptide chain and deprotection of the side chains, the linear aldehyde was released from the resin. Subsequent intramolecular heterocyclization of the C-terminal aldehyde and the N-terminal cysteine afforded the macrocycle **1** through in situ thiazolidine formation.[7] The thiazolidine, and thus **1**, exists in two interconverting and,

[*] Dr. N. A. Schilling, J. S. Saur, Dr. M. C. Konnerth, S. N. Wirtz, J. M. Beltrán-Beleña, Prof. S. Grond
Institute of Organic Chemistry, Biomolecular Chemistry
Eberhard Karls Universität Tübingen
Auf der Morgenstelle 18, 72076 Tuebingen (Germany)
E-mail: stephanie.grond@uni-tuebingen.de

Dr. A. Berscheid, Dr. A. Zipperer, Dr. B. Krismer, Prof. A. Peschel, Prof. H. Brötz-Oesterhelt
Interfaculty Institute of Microbiology and Infection Medicine
German Center for Infection research (DZIF)
Eberhard Karls Universität Tübingen
72076 Tuebingen (Germany)

J. Schumacher, Prof. C. Steinem
Institute of Organic and Biomolecular Chemistry
Georg August Universität Göttingen
37077 Goettingen (Germany)

Dr. H. Kalbacher
Interfaculty Institute of Biochemistry
Eberhard Karls Universität Tübingen
72076 Tuebingen (Germany)

Supporting information (synthesis of the peptides and procedures for the assays and vesicle experiments) and the ORCID identification numbers for the authors of this article can be found under: https://doi.org/10.1002/anie.201901589.

© 2019 The Authors. Published by Wiley-VCH Verlag GmbH & Co. KGaA. This is an open access article under the terms of the Creative Commons Attribution Non-Commercial NoDerivs License, which permits use and distribution in any medium, provided the original work is properly cited, the use is non-commercial and no modifications or adaptations are made.

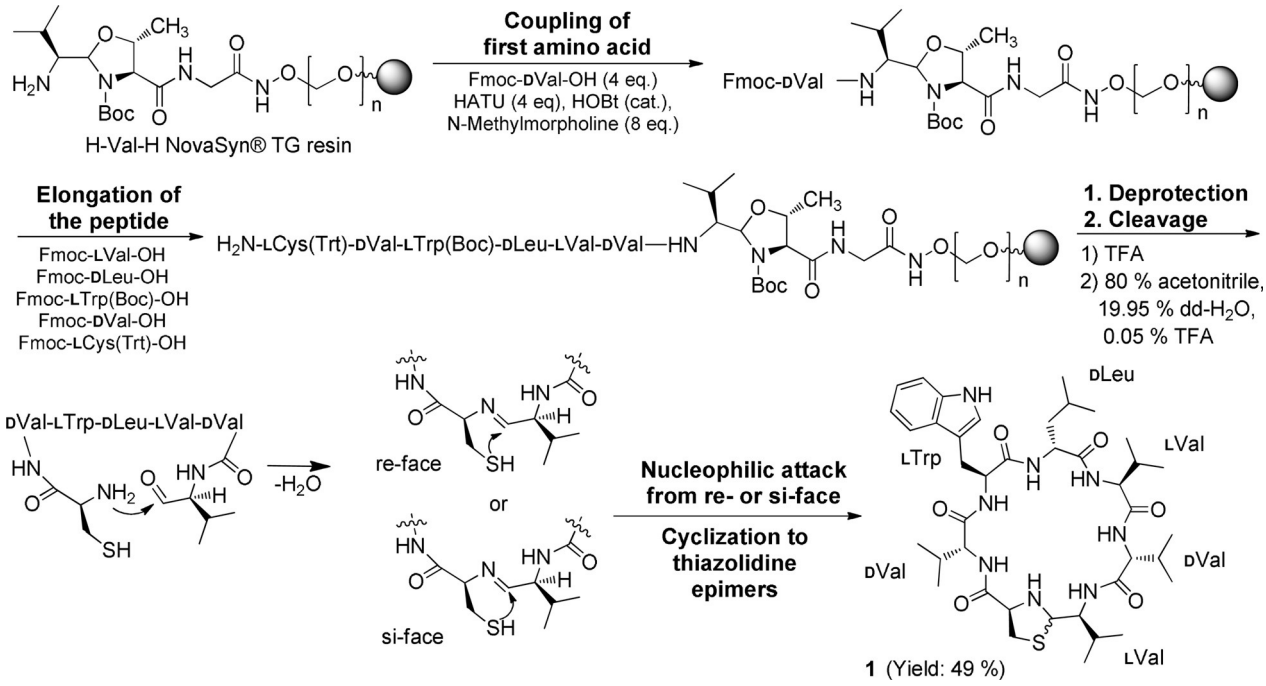

Scheme 1. Solid-phase aldehyde peptide synthesis of **1**.

therefore, inseparable epimeric forms (Scheme 1). The poor coupling of consecutive valine residues (Val^5, Val^6) was addressed by peptide elongation in acetonitrile (see Figure S1 in the Supporting Information). The optimized strategy provided access to many peptides.

All the peptides were tested as crude products for activity against the MRSA strain USA300 LAC (hereafter: USA300, Table 1). During cleavage, the aldehyde α-carbon atom of the valine residue at position 7 (Val^7, Ala^7 in **8**) of the peptides partially racemized, thereby leading to mixtures of L- and D-valine or -alanine adjacent to the thiazolidine ring (see Scheme S1 and Figure S2 in the Supporting Information). Crude peptides with significant activity (MIC $\leq 50\ \mu g\,mL^{-1}$) were purified to determine the exact MIC. We suggest terming the new class of lugdunins fibupeptides (lat. fibula, clasp) to define macrocyclic peptides with a thiazolidine moiety as an "ornament clasp".

The importance of individual amino acids for the activity of **1** was revealed by an alanine scan,[8] which yielded fibupeptides **2**–**8**. Each amino acid of **1** was successively replaced by alanine with the same stereoconfiguration. Antimicrobially inactive peptide **2** neither carries a thiazolidine nor is cyclic because of the lack of cysteine. Mass spectrometry analysis of **2** showed the formation of an aldehyde-methanol adduct ($[M+MeOH]^+$, m/z 801.5232, 0.12 Δppm). This is in agreement with the finding of Enck et al. that the precursor aldehyde of tyrocidine A did not spontaneously cyclize to the imine.[9]

Consequently, cysteine and, hence, the thiazolidine ring is essential. Active alanine peptides **3**, **6**, **7**, and **8** showed MIC values of $12.5\ \mu g\,mL^{-1}$ (16.6 μM) to $25\ \mu g\,mL^{-1}$ (33.1 μM), which is a four- to eightfold reduction in the antimicrobial activity. The most pronounced impact on antibiotic efficacy was detected for the exchange of Trp^3 (**4**) and Leu^4 (**5**) for alanine. Both derivatives showed MIC values $\geq 100\ \mu g\,mL^{-1}$ and were regarded as inactive. Therefore, tryptophan and

Table 1: MIC values of peptides **1**–**25**.

	AA sequence	Differences highlighted	MIC[a]
1	(CVWLVVV)	lugdunin (lug)	3.1 (3.9)
2	AVWLVVValinal[b]	**1-Ala**-lug	≥100
3	(CAWLVVV)	**2-Ala**-lug	12.5 (16.6)
4	(CVALVVV)	**3-Ala**-lug	≥100
5	(CVWAVVV)	**4-Ala**-lug	≥100
6	(CVWLAVV)	**5-Ala**-lug	12.5 (16.6)
7	(CVWLVAV)	**6-Ala**-lug	25.0 (33.1)
8	(CVWLVVA)	**7-Ala**-lug	25.0 (33.1)
9	(CVWLVVV)	**linear** lug (-COOH)	≥100
10	$CVWLVVV_{cycl.}$	**cyclized homodetic** lug	≥100
11	(Me-CVWLVVV)	***N*-methylthiazolidine**-lug	≥100
12	(Ac-CVWLVVV)	***N*-acetylthiazolidine**-lug	≥100
13	(*homo*CVWLVVV)	**1,3-thiazinane**-lug	≥100
14	$PVWLVVV_{cycl.}$	**1-Pro homodetic** lug	≥100
15	(CVWLVVV)	**1**-D-lug	≥100
16	(CVWLVVV)	**2**-L-lug	≥100
17	(CVWLVVV)	**3**-D-lug	≥100
18	(CVWLVVV)	**4**-L-lug	≥100
19	(CVWLVVV)	**5**-D-lug	≥100
20	(CVWLVVV)	**6**-L-lug	≥100
21	(CVWLVVV)	**7**-D-lug	≥100
22	(CVWLVVV)	**enantio**-lug	3.1 (3.9)
23	(CVWLVWV)	**6-Trp**-lug	1.6 (1.8)
24	(CPraWLVWV)	**2-Pra-6-Trp**-lug	3.1 (3.9)
25	VOLFPVOLFP$_{cycl.}$	gramicidin S	6.2 (5.4)

[a] MRSA USA300 LAC (MIC in $\mu g\,mL^{-1}$ (μM). For *S. aureus* NCTC8325 MICs, see Table S3). Single-letter codes for amino acids, brackets indicate cyclic structure (cyclization via thiazolidine), *cycl.* indicates cyclization via the peptide bond, underlined letters represent D-amino acids. [b] Detected as $[M+MeOH]^+$ by ESI-MS, Ala = alanine, Pro = proline, Trp = tryptophan, Pra = propargylglycine.

 © 2019 The Authors. Published by Wiley-VCH Verlag GmbH & Co. KGaA, Weinheim

leucine are crucial for the antibacterial activity, whereas valine versus alanine exchanges are well-tolerated. However, the different activities of **3**, **6**, **7**, and **8** imply a distinct relevance of each valine.

The importance of the thiazolidine ring was investigated, starting with the linear lugdunin peptide **9** (Figure 1). Intramolecular cyclization of **9** yielded homodetic analogue **10** in which the ring is composed exclusively of normal peptide

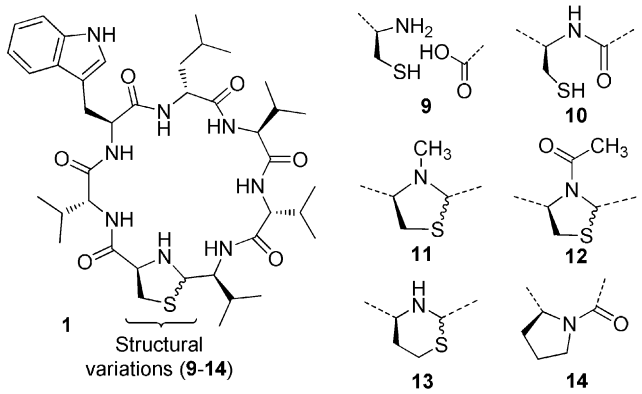

Figure 1. Structure of lugdunin (**1**) and analogues **9**–**14**.

bonds. Both peptides were inactive against USA300. In addition, the role of the thiazolidine NH proton was addressed by replacing it by a tertiary amine through methylation (**11**) and acetylation (**12**). **11** and **12** are inactive as antibacterial agents, thus demonstrating the indispensability of the secondary amine of the thiazolidine ring. We speculate that the basicity of the thiazolidine amine or its three-dimensional structure are responsible for the bioactivity of **1**. Inactive **13** was prepared with homocysteine to expand the heterocycle by an additional methylene group. The six-membered 1,3-thiazinane affects the structure of **1** adversely in terms of activity, even though it contains a secondary amine. Since the thiazolidine resembles an unusual 2-connected thioproline, we synthesized the proline-containing homodetic **14**, which was inactive. Thus, both, the thiazolidine ring and its secondary amine are essential for the antimicrobial activity of **1**.

The intriguing D-,L-architecture of **1** prompted us to conduct a stereo scan, while retaining the sequence and hydrophobic character of **1**. One amino acid at a time was incorporated as its enantiomer (**15**–**21**). All the diastereomers were ineffective against USA300, which demonstrates that any inversion of a stereogenic center dramatically affects the antimicrobial potency. To clarify whether the inversion of the absolute configuration of **1** also has such an impact on activity, we synthesized its enantiomer **22**. Remarkably, **22** showed identical antibiotic activity as **1**. This situation has been rarely discussed for natural products, for example, for the antiviral feglymycin[8] or the antibiotic lysocin E.[10] The insignificance of the absolute configuration of **1** suggests that the MoA does not depend on a stereospecific receptor–ligand interaction but could involve the recognition of achiral small molecules or ions.[10]

Together, these SAR studies revealed that an unsubstituted thiazolidine, tryptophan, leucine, and an alternating amino acid stereoconfiguration are essential structural motifs of **1**. Tryptophan and leucine are abundant in peptides that interact with bacterial cell membranes such as synthetic poly-(Trp-Leu)-octapeptides.[11] The necessity of tryptophan and leucine and the decrease in the activity of the less hydrophobic alanine fibupeptides **3**, **6**, **7**, and **8** pointed towards an interaction of **1** with the hydrophobic region of bacterial membranes.

A double tryptophan-containing fibupeptide (**23**) was designed to intensify the presumed interaction with the bacterial membrane. D-Tryptophan was incorporated (Trp^6) within the nonpolar flank ($DLeu^4$-$LVal^5$-$DVal^6$-$LVal^7$) of **1**. Fibupeptide **23** showed a twofold increased activity. As could be deduced from the alanine scan, position 2 shows tolerance for side-chain modification while retaining activity. Incorporation of D-propargylglycine (Pra) at this position in **23** resulted in active derivative **24. 24** is suitable for 1,3-dipolar cycloaddition to enable the production of further analogues, preferably with activity against Gram-negative bacteria.[12]

With the knowledge that the enantiomer (**22,** Figure 2) shows activity identical to **1**, we suspected that **1** might move achiral molecules or ions across lipid membranes. This concurs with our previous observation that bacterial cells exposed to **1** stopped incorporating radioactive DNA, RNA, protein, and cell-wall precursors.[6] Thus, the influence of the active fibupeptides **1**, **3**, **22**, and **23** on the transmembrane potential of *S. aureus* NCTC8325 was compared to that of the less active or inactive **5**, **11**, and **21**. When entering the cell, the green fluorescence of the dye $DiOC_2(3)$ shifts towards a red emission because of a self-association that depends on membrane potential.[13]

All the tested peptides affected the transmembrane potential of *S. aureus* NCTC8325, in full correlation with

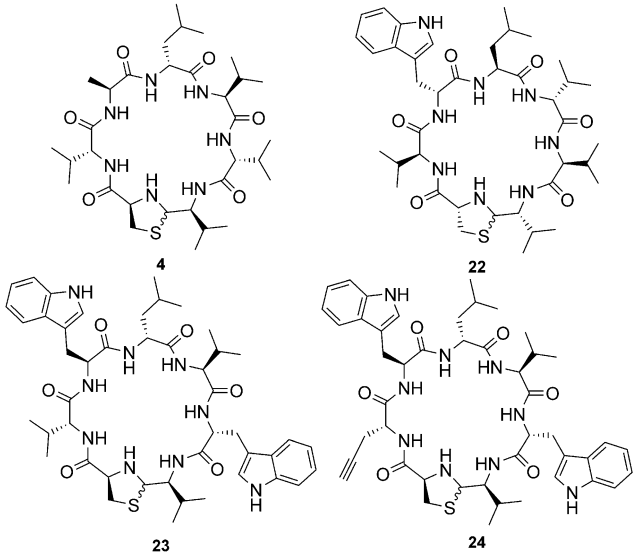

Figure 2. Exemplified derivatives of **1. 4** is an inactive alanine analogue. The enantiomer **22** shows identical activity as **1. 23** and **24** are specially designed analogues of **1** with twofold and equal activity, respectively.

 © 2019 The Authors. Published by Wiley-VCH Verlag GmbH & Co. KGaA, Weinheim

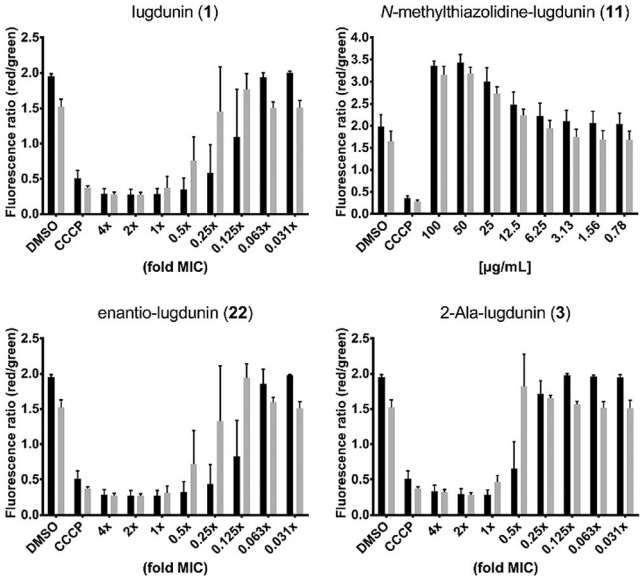

Figure 3. Effect of **1**, **11**, **22**, and **3** on the *S. aureus* NCTC8325 membrane potential after 30 (black bars) and 60 minutes (gray bars) of treatment. The protonophore CCCP (5 μM) was used as a positive and DMSO as a negative control. Error bars represent the standard deviation (SD) of two biological replicates including two technical replicates each.

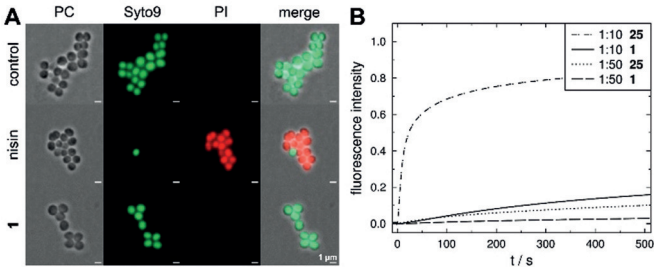

Figure 4. Complementary experiments excluding large pores or lesions. A) Fluorescence microscopy of *S. aureus* treated with pore-forming nisin (1–2 × MIC) or **1** (10 × MIC). Scale bars: 1 μm. B) Time course of normalized CF leakage from POPC vesicles, induced by **25** and **1** at concentrations of 5 μM and 1 μM (P/L 1:10 and 1:50).

their MIC values, and in a concentration-dependent manner (Figure 3, see also Figure S11 and Table S3 in the Supporting Information). Partial membrane depolarization occurred at concentrations slightly below the MIC (0.125–0.5 × MIC), while inactive **11** showed no effect. This is in accordance with the parallel cessation of all biosynthetic pathways and indicates a MoA involving impairment of membrane integrity or ion leakage/transport.

Remarkably, **1** does not tolerate amino acids with polar (Ser, Thr) or protonated (Lys) side chains without losing bioactivity—in contrast to common peptides that disrupt the membrane potential such as gramicidin A.

To analyze the effects on bacterial membranes, we treated *S. aureus* with **1** and subsequently added a mixture of the dyes Syto9 and propidium iodide (PI) to the cells as an indicator for pore formation. The red-fluorescent PI can only cross the cytoplasmic membrane through large pores or lesions. Treatment with **1** up to a concentration of 30 $\mu g\,mL^{-1}$ (10 × MIC) did not allow for PI entry into the *S. aureus* cells, while nisin led to a strong influx of the dye because of its ability to form large pores (Figure 4A).

We further employed unilamellar vesicles composed of POPC (1-palmitoyl-2-oleoyl-*sn*-glycero-3-phosphocholine) as a membrane model system to assess the activity of **1**. The use of artificial lipid bilayers enables the characterization of membrane activity independent of other factors such as proteins. We investigated first whether **1** impairs vesicle integrity.[14] The ability of **1** to induce release of the fluorescent dye carboxyfluorescein (CF) was compared to that of the cyclic decapeptide gramicidin S (**25**), which can destabilize membranes.[15] The dye is entrapped in vesicles in a self-quenching concentration (100 mM) and leakage results in an increase in fluorescence. In contrast to **25**, **1** induced only very slow leakage of the dye even at high concentrations (Figure 4B). This result supports the notion that **1** does not destabilize the membrane, but rather acts by translocating ions.

We investigated the ability of **1** to transport protons by using vesicles filled with the pH-sensitive fluorescent dye pyranine (HPTS).[16] A pH gradient was established across the lipid bilayer and proton transport was observed as a change in fluorescence. As proton translocation across a membrane induces a transmembrane potential that prevents further transport, the change in the internal pH value is also dependent on charge equilibration and, therefore, transport of further ions. A control experiment with the protonophore carbonyl cyanide *m*-chlorophenyl hydrazone (CCCP) and the potassium ionophore valinomycin showed that both ions have to be transported to explain rapid pH equilibration (see Figure S12 in the Supporting Information). Figure 5 shows that **1** causes rapid proton translocation at concentrations as low as 50 nM (peptide to lipid ratio (P/L) 1:1000) irrespective of the direction of the gradient. To exclude dye leakage, pyranine fluorescence was quenched outside the vesicles in a control experiment (see Figure S12 in the Supporting Information).

In this pH assay, **1** demonstrated a significantly higher proton translocation capability than **25**, whereas antimicrobially inactive **11** showed greatly reduced proton transport (Figure 5C). This finding suggests a vital role of the thiazolidine moiety in proton translocation and is in agreement with the membrane depolarization data.

In summary, we established an optimized synthesis of **1** to provide access to manifold analogues. By SAR studies, we revealed the essential motifs for antimicrobial activity, notably, the alternation of D- and L-amino acids, the presence of tryptophan and leucine, as well as the N-unsubstituted thiazolidine ring. The identical activity of the enantiomer **22** suggested that chiral recognition was not relevant for the MoA of **1**. Additionally, **1** and its analogues illustrate a strong correlation between membrane depolarization and MIC values with *S. aureus* cells. Furthermore, **1** did not induce large pores in either *S. aureus* cells or POPC vesicles and acts through proton translocation in synthetic membrane vesicles. In addition, the twofold more active **23** (Trp^6) verified these insights.

 © 2019 The Authors. Published by Wiley-VCH Verlag GmbH & Co. KGaA, Weinheim

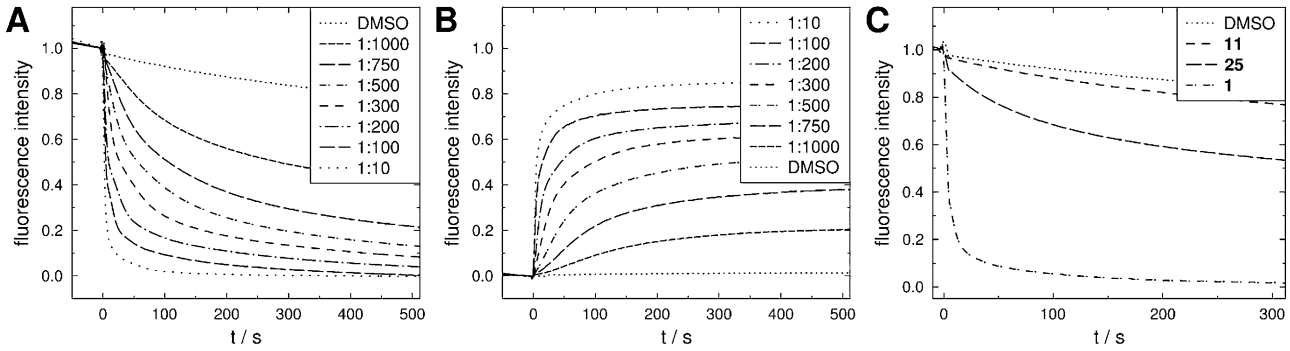

Figure 5. Time course of normalized pyranine fluorescence after addition of: A,B) 5 μM to 50 nM **1** (P/L 1:10 to 1:1000) with A) proton influx from pH 6.4 to 7.4, B) proton efflux from pH 7.4 to 8.4, C) after addition of 1 μM (P/L 1:50) **11**, **25**, and **1**, proton influx from pH 6.4 to 7.4. The vesicles were composed of POPC, total lipid concentration 50 μM containing 0.5 mM pyranine.

The active analogue **24** with a propargyl function paves the way for the production of analogues with optimized bioactivity or fluorescent properties, which will contribute to elucidating the mechanistic interaction between **1** and MRSA on the molecular level. The exact role of the vital thiazolidine ring is the focus of current investigations along with the question of whether **1** translocates protons as a mobile carrier or by channel formation.

Acknowledgements

The work of N.A.S. is supported by the Institutional Strategy of the University of Tübingen (DFG, ZUK 63). We are grateful to RTG 1708 (M.C.K., A.P., H.B.-O., S.G.) and SFB 766 (A.P., H.B.-O., S.G.) for financial support. B.K., A.P., H.B.-O., and A.B. acknowledge support through infrastructural funding from DZIF and Cluster of Excellence EXC 2124. We further acknowledge Jan Straetener and Jutta Gerber-Nolte for technical support and Pascal Rath for NMR measurements.

Conflict of interest

Eberhard Karls University Tübingen holds a patent (EP3072899B1) covering the compound lugdunin, derivatives thereof, and the bacterial infection prevention by lugdunin producing bacteria. The patent has also been filed in the USA (US2018/0155397A1).

Keywords: aldehyde peptide synthesis · methicillin-resistant *Staphylococcus aureus* · proton translocation · synthetic membrane vesicles · thiazolidine antibiotics

How to cite: *Angew. Chem. Int. Ed.* **2019**, *58*, – *Angew. Chem.* **2019**, *131*, –

[1] T. R. Walsh, *Nat. Microbiol.* **2018**, *3*, 854 – 855.
[2] S. Zhang, L. M. De Leon Rodriguez, I. K. H. Leung, G. M. Cook, P. W. R. Harris, M. A. Brimble, *Angew. Chem. Int. Ed.* **2018**, *57*, 3631 – 3635; *Angew. Chem.* **2018**, *130*, 3693 – 3697.
[3] J. Montenegro, M. R. Ghadiri, J. R. Granja, *Acc. Chem. Res.* **2013**, *46*, 2955 – 2965.
[4] S. J. Kaldas, A. K. Yudin, *Chem. Eur. J.* **2018**, *24*, 7074 – 7082.
[5] D. Janek, A. Zipperer, A. Kulik, B. Krismer, A. Peschel, *PLoS Pathog.* **2016**, *12*, e1005812.
[6] A. Zipperer, M. C. Konnerth, C. Laux, A. Berscheid, D. Janek, C. Weidenmaier, M. Burian, N. A. Schilling, C. Slavetinsky, M. Marschal, M. Willmann, H. Kalbacher, B. Schittek, H. Brötz-Oesterhelt, S. Grond, A. Peschel, B. Krismer, *Nature* **2016**, *535*, 511 – 516.
[7] L. R. Malins, J. N. deGruyter, K. J. Robbins, P. M. Scola, M. D. Eastgate, M. R. Ghadiri, P. S. Baran, *J. Am. Chem. Soc.* **2017**, *139*, 5233 – 5241.
[8] F. Dettner, A. Hänchen, D. Schols, L. Toti, A. Nußer, R. D. Süssmuth, *Angew. Chem. Int. Ed.* **2009**, *48*, 1856 – 1861; *Angew. Chem.* **2009**, *121*, 1888 – 1893.
[9] S. Enck, F. Kopp, M. A. Marahiel, A. Geyer, *Org. Biomol. Chem.* **2010**, *8*, 559 – 563.
[10] M. Murai, T. Kaji, T. Kuranaga, H. Hamamoto, K. Sekimizu, M. Inoue, *Angew. Chem. Int. Ed.* **2015**, *54*, 1556 – 1560; *Angew. Chem.* **2015**, *127*, 1576 – 1580.
[11] M. R. Ghadiri, J. R. Granja, L. K. Buehler, *Nature* **1994**, *369*, 301.
[12] P. A. Smith, et al. *Nature* **2018**, *561*, 189 – 194.
[13] D. Novo, N. G. Perlmutter, R. H. Hunt, H. M. Shapiro, *Cytometry* **1999**, *35*, 55 – 63.
[14] J. N. Weinstein, R. D. Klausner, T. Innerarity, E. Ralston, R. Blumenthal, *Biochim. Biophys. Acta Biomembr.* **1981**, *647*, 270 – 284.
[15] M. Wenzel, M. Rautenbach, J. A. Vosloo, T. Siersma, C. H. M. Aisenbrey, E. Zaitseva, W. E. Laubscher, W. van Rensburg, J. C. Behrends, B. Bechinger, L. W. Hamoen, *mBio* **2018**, *9*, e00802-18.
[16] K. Kano, J. H. Fendler, *Biochim. Biophys. Acta Biomembr.* **1978**, *509*, 289 – 299.

Manuscript received: February 6, 2019
Revised manuscript received: March 13, 2019
Accepted manuscript online: May 6, 2019
Version of record online: May 27, 2019

 © 2019 The Authors. Published by Wiley-VCH Verlag GmbH & Co. KGaA, Weinheim